Supporting Information

A melanin-inspired robust aerogel for multifunctional water remediation

Peng Yang,[1] Wanjie Bai [1], Yuan Zou,[1] Xueqian Zhang, [1] Yiyan Yang,[1] Gaigai Duan,[2] Jinrong Wu[1], Yuanting Xu[1,] and Yiwen Li[1,*]*

1- College of Polymer Science and Engineering, State Key Laboratory of Polymer Materials Engineering, Sichuan University, Chengdu 610065, China.

2- Jiangsu Co-Innovation Center of Efficient Processing and Utilization of Forest Resources, International Innovation Center for Forest Chemicals and Materials, College of Materials Science and Engineering, Nanjing Forestry University, Nanjing 210037, China.

E-mail: ywli@scu.edu.cn (Y.L.), Tel: +86 028-85401066; xuyt@scu.edu.cn (Y.X.), Tel: +86 028-85401066.

Adsorption Measurement

The adsorption measurements were conducted with a shaking speed of 100 rpm (temperature: ~25 °C and humidity: ~55%). Organic dyes (MB and Rh B) and heavy metal ions (Cu^{2+}, Cd^{2+}, Cr^{3+} and Ni^{2+}) were selected as model contaminants to test the adsorption performance of the aerogel. Initially, dye and heavy metal ion aqueous solutions were prepared in different concentrations. Then, the aerogel (20 mg ± 2 mg) was allotted to each dye and heavy metal ion solution (25 mL) followed by shaking in dark over 24 h to reach the adsorption equilibrium. The contents of MB and Rh B in aqueous solutions were measured at fixed time intervals by using a UV-vis spectrometer (Shimadzu UV3600), which could be evaluated by the absorbance at 665 nm (MB) and 555 nm (Rh B). The metal ions concentrations were determined using inductively coupled plasma atomic emission spectroscopy (ICP-AES). The experiments were repeated three times.

The adsorption abilities of the aerogel at equilibrium were calculated according to the following equation:

$$Q_e = (C_0 - C_e)V/m \quad (1)$$

where C_0 is the initial concentration (mg L^{-1}) of dyes and heavy metal ions contaminants, C_e is the concentration of dyes and heavy metal ions at equilibrium, m is the amount of the aerogel (g), and V is the volume of the aqueous solution (L).

Furthermore, to measure the adsorption isotherm, dyes and heavy metal ions adsorption

experiments were carried out in aqueous solutions with different concentrations ranging from 10 to 200 mg/L and 10 to 500 mg/L, respectively. Two models were used to fit the isotherm datum as follows:

Langmuir model:

$$\frac{C_e}{Q_e} = \frac{C_e}{Q_m} + \frac{1}{bQ_m} \quad (2)$$

where Q_m (mg g^{-1}) is the maximum adsorption amount, Q_e (mg g^{-1}) is the amount of dye and heavy metal contaminants adsorbed by the aerogel at equilibrium, b represents the equilibrium constant of the adsorption reaction (L mg^{-1}).

Freundlich model:

$$\ln Q_e = \ln k + \frac{1}{n} \ln C_e \quad (3)$$

where k and n are the Freundlich constants, k is roughly an indicator of the adsorption capacity (mg g^{-1}), and $1/n$ is an empirical parameter related to the adsorption intensity.

We also tested the kinetics of the aerogel adsorbing dyes and heavy metal ions. The initial concentration of both dye and heavy metal ions was 10 mg L^{-1}. The time-dependent concentrations of both dye and heavy metal ions were measured as above. The relationship between the adsorption amount (Q_t) and time (t) was calculated by the following equation:

$$Q_t = (C_0 - C_t)V/m \quad (4)$$

where C_0 is the initial concentration (mg L^{-1}) of dye and heavy metal ions contaminants, C_t is the concentration of dye and heavy metal contaminants at a certain time, m is the amount of the aerogel (g), and V is the volume of the aqueous solution (L). The kinetic study data was fitted to models as follows:

Pseudo-first-order kinetic equation:

$$-\ln(1 - Q_t/Q_e) = k_1 t + C \quad (5)$$

where Q_e and Q_t are the amounts of the metal ions adsorbed (mg g^{-1}) at equilibrium and t time (min), and k_1 (min^{-1}) is the pseudo-first-order adsorption rate constant.

Pseudo-second-order kinetic equation:

$$\frac{t}{Q_t} = \frac{1}{k_2 Q_e^2} + \frac{t}{Q_e} \quad (6)$$

where k_2 (g mg^{-1} min^{-1}) is the rate constant of the pseudo- second-order adsorption reaction.

Simulation Method

Molecular dynamics (MD) MD simulation was performed using the amorphous cell module of Materials Studio (Accelrys Software Inc.) with a dreiding force field whose intermolecular parameters were optimized using quantum mechanics. A parent aerogel with a five-generation dendrimer was built that consists of indole and hydroxyl groups. Although size of the parent aerogel chain is not sufficiently long to represent conformations of a real polymer chain, a previous study has reported a good agreement

between experiments and simulations when simulated Li-CMP chains are short (merely five-generation dendrimer on average).[1] Moreover, a periodic boundary condition were imposed and an initial density of 0.9 g/cm^3 was used to simulate the polymer conformation in bulk under an equilibrium state. The aerogel dendrimer in simulation box was relaxed through NVT for 1 ns at 800 K with time steps of 0.2 fs. The simulation of high-temperature relaxation was closely followed a protocol S9 suggested previously.[2] After 1 ns of simulated relaxation at 800 K, the system temperature is decreased to 273 K. In order to obtain a suitable structure for further analysis, ten different initial structures for each system were built and relaxed according to the procedure mentioned previously. The one with the lowest system energy was selected as the MD result for further analysis. The MD simulation was performed to analyze the conformation of the complex between the aerogel and metal ions under an equilibrium state. For example, it is clear that the M^+ cation is close to an indole group. To see this in a quantitative way, the radial distribution function, $g_{AB}(r)$, was introduced to describe how density of designated particles varies as a function of distance from a reference particle. Usually, $g_{AB}(r)$ is determined by measuring the ensemble averaged distance between all particle pairs, as follows:

$$g_{AB}(r) = \frac{\langle n_{AB}(r) \rangle}{4\pi r^2 \Delta\rho_{AB}} \quad (7)$$

where, $n_{AB}(r)$ is the distance of each pair between A (M^+) and B (indole) in the simulation box. <...> represents an ensemble average. $\Delta\rho_{AB}$ is the rate of change in the average number density of M^+ over distance from an indole ring. The plot of $g_{AB}(r)$

gives the local density of B around A at a distance r. $g_{AB}(r) = 1$ indicate the particles are completely uncorrelated. A positive peak of $g_{AB}(r)$ reflects a definite correlation between atoms at r. In addition, the complexation also confirmed by the same calculation methods.

Density functional theory (DFT) The molecules were optimized with density functional theory (DFT) at the M062x/6-311+g** level theory, using the Gaussian-09 package. The electrostatic potential (ESP) of the model were analyzed using Multiwfn 3.3.5.[3] The simulation procedure was closely followed a previously suggested one.[4]

Figure S1. Schematic illustration of the aerogel fabrication strategy.

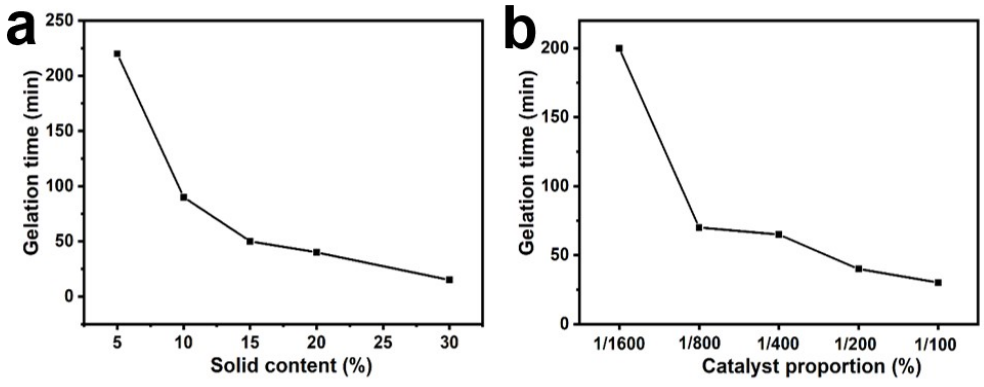

Figure S2. Gelation time of hydrogels with different (a) solid contents (NaOH : DHI = 1 : 200) and (b) catalyst proportions (solid content = 20%).

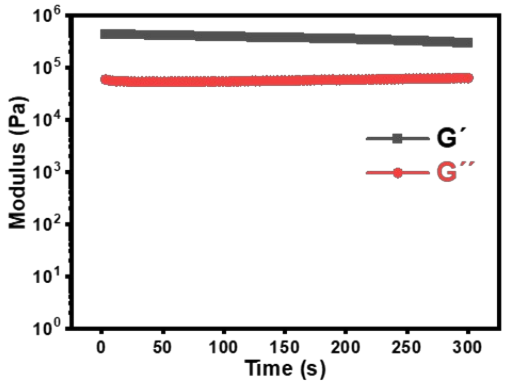

Figure S3. Time-dependent rheology measurement of the model hydrogel conducted at 1% strain and an angular frequency of 10 rad/s.

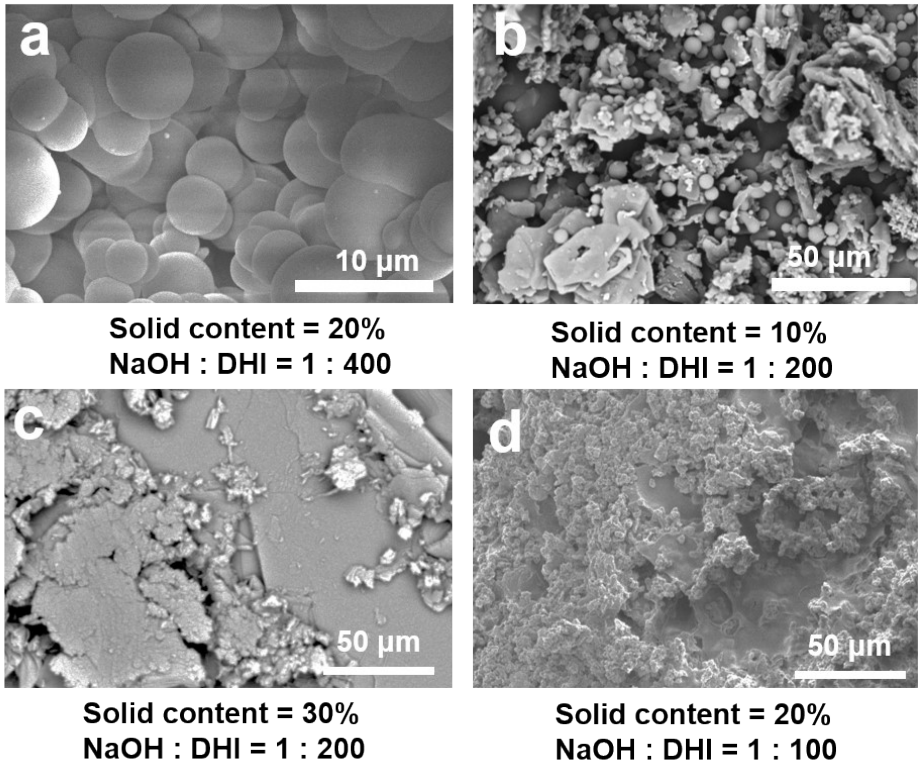

Figure S4. SEM images of the aerogels under various preparation conditions.

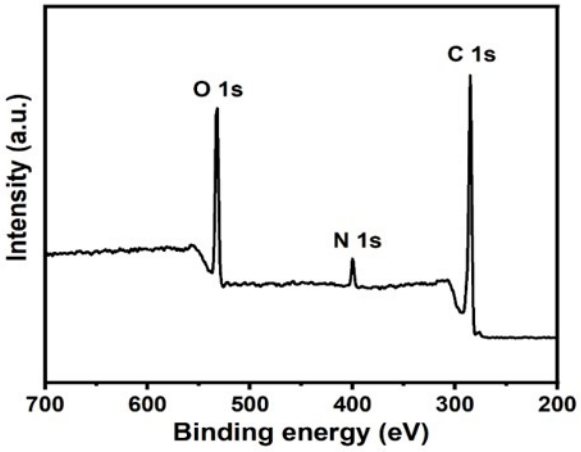

Figure S5. XPS spectrum of the aerogel.

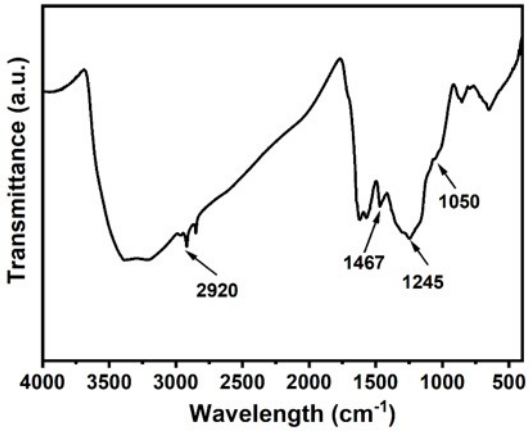

Figure S6. FTIR spectrum of the aerogel.

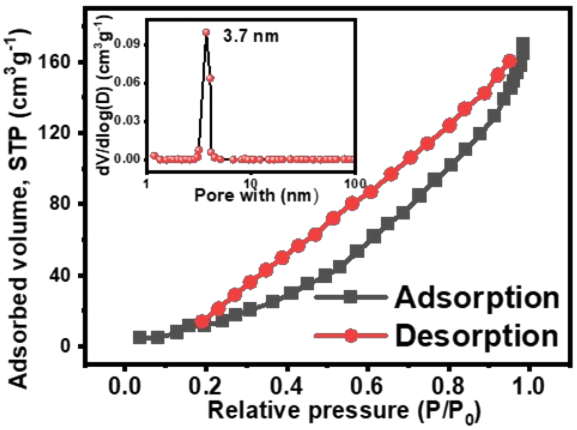

Figure S7. Nitrogen adsorption–desorption isotherms and the pore size distribution (inset) of the aerogel.

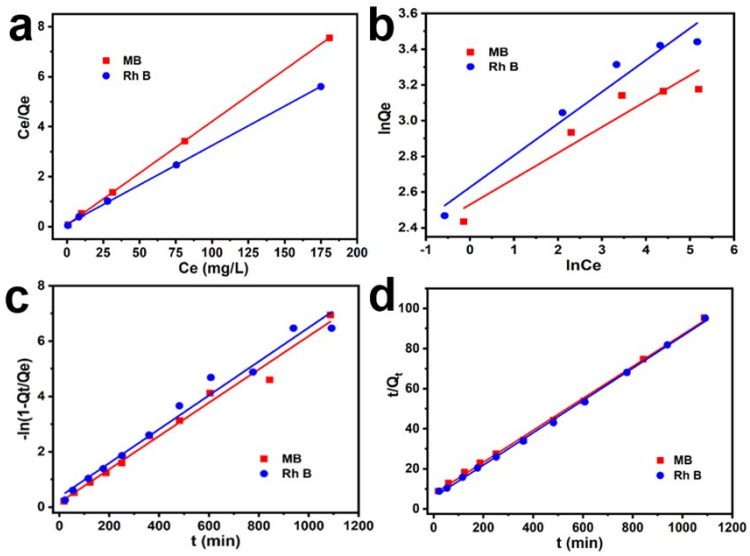

Figure S8. (a) Linear fitting curves with the Langmuir model, (b) linear fitting curves with the Freundlich model, (c) the simulated pseudo-first-order kinetics, (d) the simulated pseudo-second-order kinetics for organic dyes.

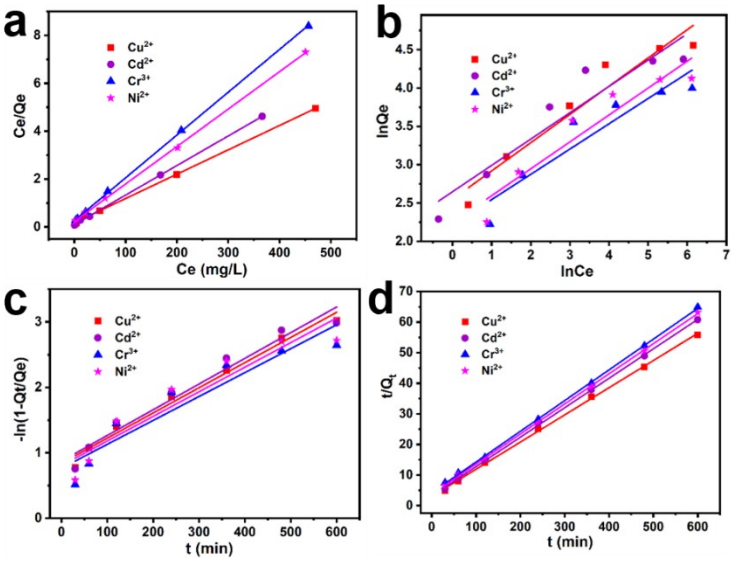

Figure S9. (a) Linear fitting curves with the Langmuir model, (b) linear fitting curves with the Freundlich model, (c) the simulated pseudo-first-order kinetics, (d) the simulated pseudo-second-order kinetics for heavy metal ions.

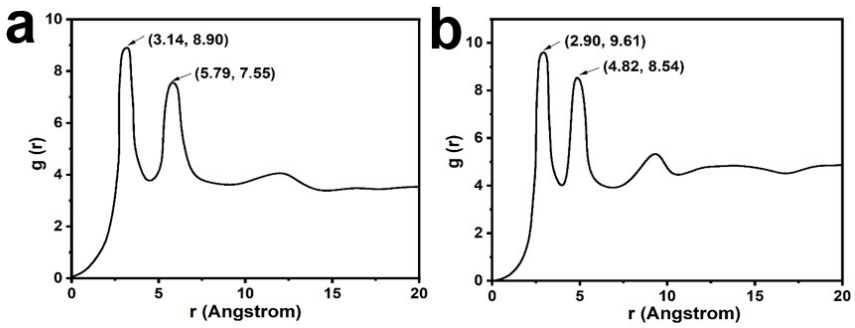

Figure S10. RDF of (a) Cu^{2+} to the distance of the indole groups and (b) Cu^{2+} to the distance of the indole OH groups.

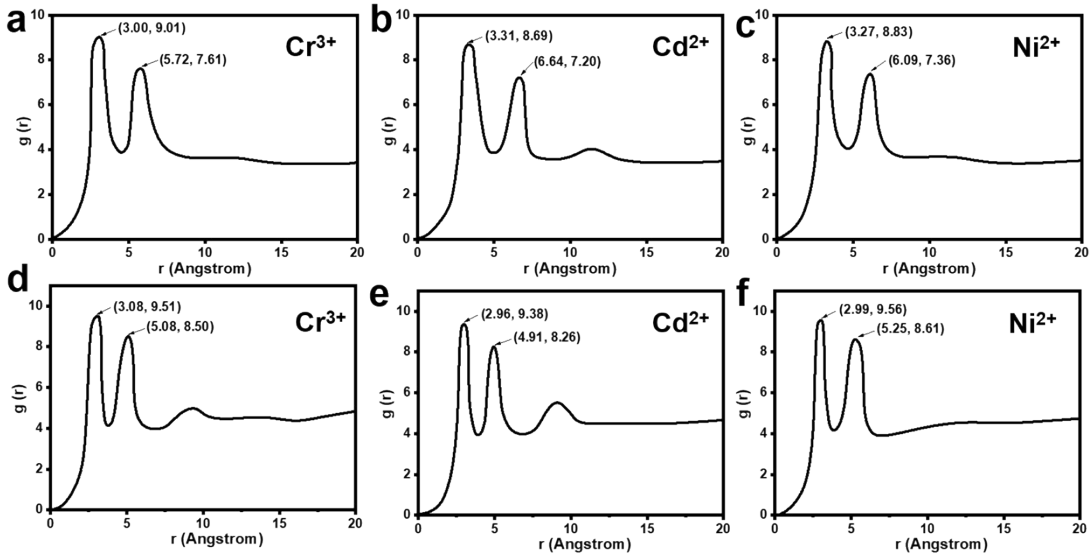

Figure S11. RDF of (a) Cr^{3+} (b) Cd^{2+} (c) Ni^{2+} to the distance of the indole groups and (d) Cr^{3+} (e) Cd^{2+} (f) Ni^{2+} to the distance of the indole OH groups.

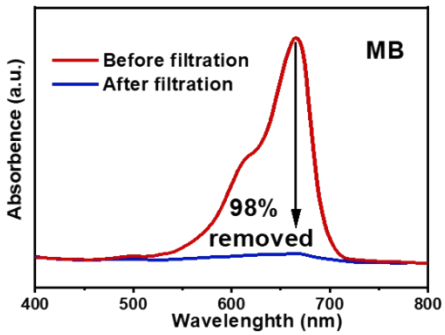

Figure S12. UV-vis spectra of the aqueous solutions before and after filtration process.

Table S1. Adsorption constants of Langmuir and Freundlich models for the adsorption of organic dyes and heavy metal ions by the aerogel.

Fitting model	Adsorption constants	Cu^{2+}	Cd^{2+}	Cr^{3+}	Ni^{2+}	MB	Rh B
Langmuir	Q_m (mg g^{-1})	98.3	81.0	56.0	64.0	24.2	31.8
	b (L mg^{-1})	0.0610	0.1334	0.0685	0.0689	0.5706	0.3293
	R^2	0.99912	0.99973	0.9998	0.99973	0.99988	0.99952
Freundlich	k (mg g^{-1})	12.8	14.1	9.2	9.4	12.6	13.8
	n	2.7150	2.9121	3.0341	2.8490	6.9070	5.6139
	R^2	0.91866	0.87267	0.8534	0.87493	0.88445	0.94882

Table S2. Parameters of two kinetic models for the adsorption of organic dyes and heavy metal ions by the aerogel.

Kinetic model	Kinetic constants	Cu^{2+}	Cd^{2+}	Cr^{3+}	Ni^{2+}	MB	Rh B
Pseudo-first-order	Q_e (mg g^{-1})	10.04	9.36	9.23	9.00	11.2	11.5
	k_1 (min^{-1})	0.00384	0.00393	0.00365	0.00376	0.00602	0.00612
	R^2	0.97941	0.9526	0.87094	0.88248	0.98239	0.9769
Pseudo-second-order	k_2 (g mg^{-1} min^{-1})	0.00261	0.00295	0.00239	0.00257	0.000863	0.001117
	Q_e (mg g^{-1})	11.26	10.40	9.96	10.17	12.56	12.42
	R^2	0.99887	0.99941	0.99964	0.99972	0.9979	0.99879

Table S3. Summary and comparison of solar-driven vapor generation performances under one sun illumination, where E.R. and η are water evaporation rate and energy efficiency, respectively.

Evaporator	Contaminants adsorption	Oil/water separation	Degree of preparation complexity	E.R. (kg m^{-2} h^{-1})	η (%)	Year	Ref.
Cellulose nanofibers-melanin hybrids	can't	can't	2 steps	1.23	78	2022	5
CG@MPT-h IPN Composite Sponge	can't	can't	3 steps	1.13	79	2021	6
CS/BFs/C@MOF sponge	can	can't	4 steps	1.481	87	2022	7
Fe^{III}/TA coated cellulose foam	can't	can't	3 steps	~1.3	77.2	2021	8
Wood-derived aerogel	can	can't	3 steps	1.25	86	2021	9
PDA@Mxene membrane	can	can	5 steps	1.276	85.2	2020	10
PDA-filled cellulose aerogel	can	can't	3 steps	1.36	86	2021	11
MXene/Carbon nanotubes/Cotton fabric	can	can't	5 steps	1.35	65	2021	12
The melanin-based aerogel	can	can	2 steps	1.42	91	This work	

CG@MPT-h IPN: chitosan/gelatin@melanin-TiO2 network, CS/BFs/C@MOF: chitosan/bamboo fibers/biochar@Zr-MOF, TA: tannic acid, PDA: polydopamine

References

1. A. Li, R. F. Lu, Y. Wang, X. Wang, K. L. Han and W. Q. Deng, *Angew. Chem. Int. Ed.*, 2010, **122**, 3402-3405.
2. K. J. Lee, W. L. Mattice and R. G. Snyder, *J.chem. phys.*, 1992, **96**, 9138-9143.
3. T. Lu and F. Chen, *J. Comput. Chem.*, 2012, **33**, 580-592.
4. T. Lu and F. Chen, *J. Mol. Graph. and Model.*, 2012, **38**, 314-323.
5. W. Yang, P. Xiao, F. Ni, C. Zhang, J. Gu, S.-W. Kuo, Q. Liu and T. Chen, *Nano Energy*, 2022, **97**, 107180.
6. X. Wang, Z. Li, Y. Wu, H. Guo, X. Zhang, Y. Yang, H. Mu and J. Duan, *ACS Appl. Mater. Interfaces*, 2021, **13**, 10902-10915.
7. X. Sun, X. Jia, H. Weng, J. Yang, S. Wang, Y. Li, D. Shao, L. Feng and H. Song, *Sep. Purif. Technol.*, 2022, **301**, 122010.
8. Y. Zou, X. Wu, H. Li, L. Yang, C. Zhang, H. Wu, Y. Li and L. Xiao, *Carbohyd. Polym.*, 2021, **254**, 117404.
9. T. Meng, B. Jiang, Z. Li, X. Xu, D. Li, J. Henzie, A. K. Nanjundan, Y. Yamauchi and Y. Bando, *Nano Energy*, 2021, **87**, 106146.
10. X. Feng, Z. Yu, R. Long, Y. Sun, M. Wang, X. Li and G. Zeng, *Sep. Purif. Technol.*, 2020, **247**, 116945.
11. Y. Zou, J. Zhao, J. Zhu, X. Guo, P. Chen, G. Duan, X. Liu and Y. Li, *ACS Appl. Mater. Interfaces*, 2021, **13**, 7617-7624.
12. Y. Wang, Q. Qi, J. Fan, W. Wang and D. Yu, *Sep. Purif. Technol.*, 2021, **254**, 117615.